

# STUDENT SUMMER INTERNSHIP TECHNICAL REPORT

## **Effects of Base Treatment and Redox Conditions on Mineral Dissolution**

DOE-FIU SCIENCE & TECHNOLOGY  
WORKFORCE DEVELOPMENT PROGRAM

Date submitted:

October 31, 2016

Principal Investigators:

Silvina A. Di Pietro (DOE Fellow Student)  
Florida International University

Dr. Hilary P. Emerson (Postdoctoral Fellow)  
Florida International University

Dr. Jim Szecsody, Mentor  
Pacific Northwest National Laboratory

Florida International University Program Director:

Leonel Lagos Ph.D., PMP®

Submitted to:

U.S. Department of Energy  
Office of Environmental Management  
Under Cooperative Agreement # DE-EM0000598

### **DISCLAIMER**

This report was prepared as an account of work sponsored by an agency of the United States government. Neither the United States government nor any agency thereof, nor any of their employees, nor any of its contractors, subcontractors, nor their employees makes any warranty, express or implied, or assumes any legal liability or responsibility for the accuracy, completeness, or usefulness of any information, apparatus, product, or process disclosed, or represents that its use would not infringe upon privately owned rights. Reference herein to any specific commercial product, process, or service by trade name, trademark, manufacturer, or otherwise does not necessarily constitute or imply its endorsement, recommendation, or favoring by the United States government or any other agency thereof. The views and opinions of authors expressed herein do not necessarily state or reflect those of the United States government or any agency thereof.

## ABSTRACT

---

DOE Fellow, Silvina A. Di Pietro, completed a 10-week internship with Pacific Northwest National Laboratory (PNNL) in Richland, Washington State. Under the mentorship of Dr. Jim Szecsody, she studied the dissolution of seven different pure minerals undergoing different types of base treatment as a potential remediation technique for uranium in the Hanford vadose zone. The objective was to develop an understanding of the kinetics of mineral dissolution following treatment with ammonium hydroxide or sodium hydroxide under variable redox conditions as a step in identifying the effects of basic treatments on the subsurface during injection. The intern received guidance on measuring ferrous iron and uranium (VI), setting up batch experiments, and using laboratory instruments, such as the Hach spectrophotometer for ferrous iron analysis. In addition, Ms. Di Pietro received invaluable guidance in experimental design and development that will benefit ongoing research endeavors.

## TABLE OF CONTENTS

---

ABSTRACT.....	iii
TABLE OF CONTENTS.....	iv
LIST OF FIGURES .....	v
LIST OF TABLES .....	vi
1. INTRODUCTION .....	1
2. EXECUTIVE SUMMARY .....	3
3. RESEARCH DESCRIPTION.....	4
4. RESULTS AND ANALYSIS.....	12
5. CONCLUSION.....	22
6. REFERENCES .....	23
APPENDIX A.....	24
APPENDIX B .....	25
APPENDIX C .....	28

## LIST OF FIGURES

Figure 1. Map of Hanford Site, Washington State [4].	1
Figure 2. Schematic diagram of waste discharges to the Hanford Site vadose zone.	2
Figure 3. Mineral grinding.	6
Figure 4. Twenty glass bottles containing different Hanford minerals about to be capped with aluminum and septa for mineral dissolution experiment.	8
Figure 5. Hach DR/4000 U spectrophotometer.	9
Figure 6. Structure of ferrozine.	10
Figure 7. Ferrous ion standards used for ferrozine colorimetric analysis for iron phase extraction.	10
Figure 8. Air-stripping technique for uranium-containing bottles N and O, with muscovite and montmorillonite respectively, with compressed air to reach neutral pH.	11
Figure 9. Si leaching ( $\mu\text{M/g}$ ) versus time (log hr) for illite.	12
Figure 10. Si leaching ( $\mu\text{M/g}$ ) versus time (log hr) for epidosite.	13
Figure 11. Si leaching ( $\mu\text{M/g}$ ) versus time (log hr) for muscovite.	14
Figure 12. Si leaching ( $\mu\text{M/g}$ ) versus time (log hr) for montmorillonite.	15
Figure 13. Mineral comparison of Si in anaerobic-DIW- $\text{NH}_4\text{OH}$ treatment condition as respect with time (log scale).	16
Figure 14. Anaerobic SGW + 1ppm + bottle L in the presence of muscovite.	17
Figure 15. Anaerobic SGW + 1ppm+ bottle M in the presence of montmorillonite.	17
Figure 16. Ferrous ion / ferric ion ratio for extract 3 (5 M HCl) and extract 5 (0.25 M dithionite-citrate-bicarbonate).	18
Figure 17. Total Iron for extract 3 (5 M HCl) and extract 5 (0.25 M dithionite-citrate-bicarbonate).	19
Figure 18. Ferric Iron - extract 3 (5 M HCl) and extract 5 (0.25 M dithionite-citrate-bicarbonate).	19
Figure 19. Ferrous Iron (ppm) for all minerals analyzed in extract 1-5.	20
Figure 20. Bottles N (blue) and O (orange) containing 3.1 M $\text{NH}_4\text{OH}$ (5% $\text{NH}_3$ ) solution air-stripped with compressed air to reach neutral pH as a function of time.	21
Figure 21. Sample magnesium calibration curve for mineral dissolution ran by ICP analysis.	25
Figure 22. Sample of total iron calibration curve and its equation of the line for iron phase extraction analysis.	27
Figure 23. Sample of total iron calibration curve to determine limit of detection based on calibration curve from Figure 22.	27
Figure 24. National Historic Landmark Nuclear Production Plant <i>B-reactor</i> constructed in 1943-1944.	28
Figure 25. Silvina at B-reactor's control room and signs around the national landmark.	29
Figure 26. With Dr. Jim Szecsody, lead scientist at the PNNL environmental system group, in his lab.	30
Figure 27. With Dr. Nik Qafoku, chief senior scientist of PNNL's geosciences group, in his lab.	30
Figure 28. Silvina at PNNL's main entrance.	31

## LIST OF TABLES

---

Table 1. Minerals Used in Dissolution and Iron Phase Extraction Experiments, Hanford Site Percent by Weight and Average Bulk Fraction of Minerals in the 200 Area Hanford and Ringold Formations [3,6-7] .....	5
Table 2. Minerals' BET Surface Area and Pore Size .....	5
Table 3. Hanford Site Synthetic Groundwater Constituents.....	7
Table 4. Conditions and Sampling Events for Seven Hanford Site Minerals for Kinetic Dissolution Experiments (Note: letters represent the labels used for sample bottles).....	8
Table 5. Reagent, Mixing Times and Target Phase for Iron Phase Extractions Extract 1-5 of Six Pure Minerals for Analyzed Species [11] .....	10
Table 6. Post Experiments BET Analysis.....	16
Table 7. Average pH for Mineral Dissolution Experiment Bottles A-T.....	24
Table 8. Standard Concentration and Average Intensity for Magnesium Calibration Curve.....	26

## 1. INTRODUCTION

The objective of this internship was to develop an understanding of the prior and ongoing research related to the treatment of the deep vadose zone using ammonia gas by working with some of the PNNL scientists most familiar with the project. The experience gained will be directly applied to advancing the ongoing research at FIU-ARC.

The Hanford Site is currently investigating the potential for ammonia ( $\text{NH}_3$ ) gas injection for remediation of uranium (U). Figure 1 shows a map of the site located in Washington State. For this effort,  $\text{NH}_3$ (gas) would be used to manipulate the pH of the system, initiating adsorption and co-precipitation processes to immobilize U.

As Figure 2 illustrates, more than 200,000 kg of U have been released to the Hanford vadose zone due to improper disposal and leakage of waste generated as a byproduct of plutonium production during World War II and the Cold War [1]. U is highly mobile due to the presence of carbonates and oxidizing conditions with a  $K_d$  of 0.11 – 8 mL/g at pH 8 [1,2].

The cleanup effort is further complicated by the deep vadose zone (up to 255 ft.) with contamination measured down to 155 ft. [3].  $\text{NH}_3$ (gas) injection is considered to be a favorable remediation technique because it is an *in situ* method that will not introduce additional liquid that could drive contaminants deeper into the vadose zone towards the groundwater table.

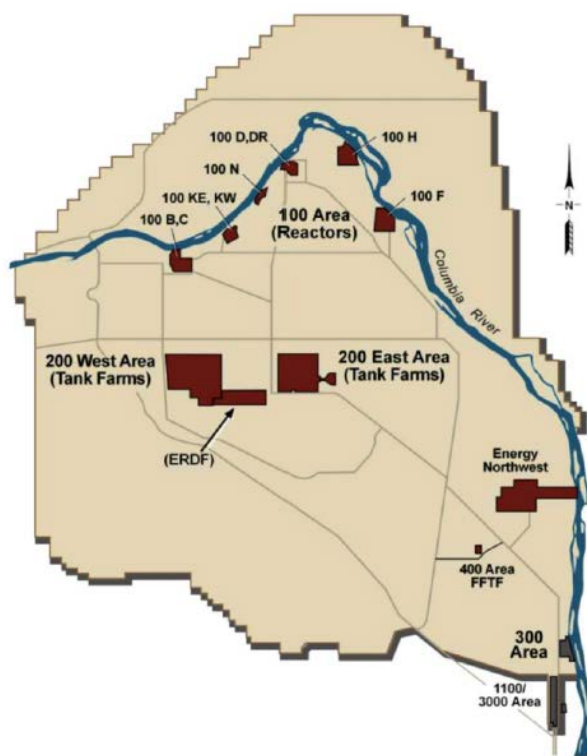


Figure 1. Map of Hanford Site, Washington State [4].

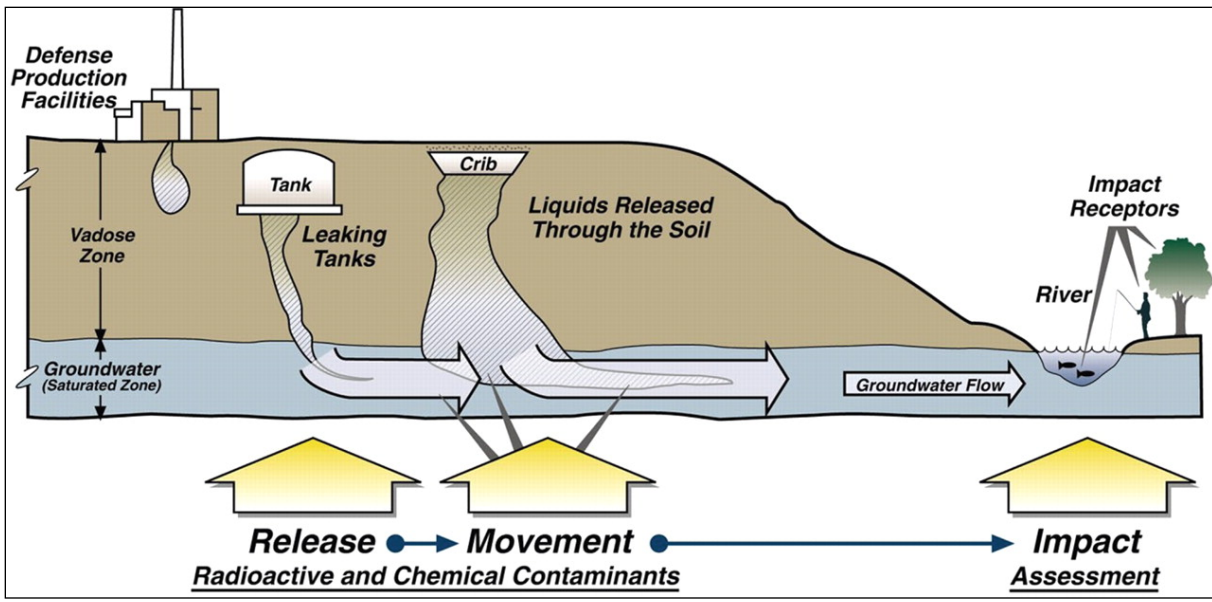


Figure 2. Schematic diagram of waste discharges to the Hanford Site vadose zone.



## **2. EXECUTIVE SUMMARY**

---

This research has been supported by the DOE-FIU Science & Technology Workforce Initiative, an innovative program developed by the US Department of Energy's Office of Environmental Management (DOE-EM) and Florida International University's Applied Research Center (FIU-ARC). During the summer of 2016, DOE Fellow Silvina A. Di Pietro spent 10 weeks participating in a summer internship experience at Pacific Northwest National Laboratory (PNNL) in Richland, WA under the supervision and guidance of Dr. Jim Szecsody, a Senior Scientist with the Environmental Systems Group. The intern's project was initiated on June 6, 2016, and continued through August 12, 2016 with the objective of performing research and assisting with experiments related to the remediation of uranium in the 200 Area of the Hanford Site in Washington State.

### 3. RESEARCH DESCRIPTION

---

#### *Objectives*

The objective of this research is to understand the mineral dissolution/kinetics of seven different minerals readily found at the Hanford Site and to quantify the redox capacities based on the Fe (II) to Fe (III) ratios in iron phase extractions.

Batch dissolution experiments were conducted using pure minerals having a significant importance at the Hanford Site 200 Area. Selected minerals are expected to dissolve under alkaline pH following *in situ* base treatment and may be an important factor controlling U mobility due to its release of ions. In addition, iron phase extractions were performed to quantify available Fe(II) and total Fe in six pure minerals. Iron is an important sorbent for many cationic metals. Further, the ratio of iron II to III can indicate the redox conditions in the subsurface. This can contribute to a better understanding of the contaminant transport at the site. Lastly, select samples treated with the weak base ammonium hydroxide were also stripped with air to remove ammonia as a gas phase. This allowed for the investigation of the effects of the pH increase followed by re-equilibration back to neutral pH as would be expected with ammonia gas treatment in the vadose zone.

#### *Materials*

##### Mineral samples

Table 1 summarizes the minerals used in both batch experiments and iron phase extractions. The first seven minerals were used for the mineral dissolution experiment to undergo five different conditions. Calcite and epidosite were crushed with a mortar and pestle (Figure 3). The mica group minerals (muscovite and biotite) were blended (Black+Decker 10-speed). The minerals were then sieved using a Cole-Parmer Sieve No. 20 to obtain a clay-size of less than 84  $\mu\text{m}$ . For the iron phase extractions, the remaining two minerals were used plus illite, montmorillonite, muscovite, and epidosite.

**Table 1. Minerals Used in Dissolution and Iron Phase Extraction Experiments, Hanford Site Percent by Weight and Average Bulk Fraction of Minerals in the 200 Area Hanford and Ringold Formations [3, 6-7]**

Experiment	Mineral	Formula	Hanford fm (% wt)	Bulk Fraction
Mineral Dissolution	Quartz	SiO <sub>2</sub>	38 ± 12	5-10
	Microcline	KAlSi <sub>3</sub> O <sub>8</sub>	15 ± 4	<5
	Calcite	CaCO <sub>3</sub>	2 ± 2	15-20
	Illite	(Al,Mg,Fe) <sub>2</sub> (Si,Al) <sub>4</sub> O <sub>10</sub> [(OH) <sub>2</sub> ,(H <sub>2</sub> O)]	2 ± 3	15-40
	Montmorillonite	(Na,Ca) <sub>0.33</sub> (Al,Mg) <sub>2</sub> (Si <sub>4</sub> O <sub>10</sub> )(OH) <sub>2</sub> · nH <sub>2</sub> O		30-35
	Muscovite	KAl <sub>2</sub> (Si <sub>3</sub> AlO <sub>10</sub> )(OH) <sub>2</sub>	2 ± 3	
Iron Phase Extractions	Epidosite	{Ca <sub>2</sub> } {Al <sub>2</sub> Fe <sup>3+</sup> } [O OH SiO <sub>4</sub>  Si <sub>2</sub> O <sub>7</sub> ]		
	Biotite	K(Mg,Fe <sup>2+</sup> <sub>3</sub> )(Al,Fe <sup>3+</sup> )Si <sub>3</sub> O <sub>10</sub> (OH,F) <sub>2</sub>		
	Magnetite	Fe <sub>3</sub> O <sub>4</sub>	5 ± 4	

**Table 2. Minerals' BET Surface Area and Pore Size**

Mineral	Average BET surface area, m <sup>2</sup> /g	Average BET pore size, Å
Quartz	0.143	106
Microcline	0.060	225
Illite	5.89	153
Montmorillonite	9.82	104
Muscovite	0.669	211
Calcite	0.174	90.1
Epidosite	0.696	101



**Figure 3. Mineral grinding.**

#### Solutions for Batch Mineral Dissolution Experiments

- Baseline solution, anaerobic (inside glovebox, de-gassed) condition: to achieve a 3.1 M  $\text{NH}_4\text{OH}$  (~5%  $\text{NH}_3$ ) solution, 171 mL of concentrated 14.5 M  $\text{NH}_4\text{OH}$  were diluted to a final volume of 780 mL with distilled deionized water ( $> 18 \text{ M}\Omega\cdot\text{cm}$ , DDI  $\text{H}_2\text{O}$ ).
- Aerobic (atmospheric temperature and pressure) condition: 53.5 mL of concentrated 14.5 M  $\text{NH}_4\text{OH}$  for a final volume amount of 240 mL.
- Anaerobic synthetic groundwater (SGW) + 1 ppm uranium (U) + 3.1 M  $\text{NH}_4\text{OH}$  (5%  $\text{NH}_3$ ) and anaerobic comparison with NaOH:
  - Synthetic groundwater: prepared synthetic groundwater (SGW) based on Table 3 below.
  - Base and U were added to SGW to achieve a concentration of 1 ppm and a pH of ~12.5. Ammonium hydroxide was added as a base treatment to the samples to reach a concentration of 3.1 M and sodium hydroxide was added to select samples to reach a concentration of 0.01 M.

**Table 3. Hanford Site Synthetic Groundwater Constituents**

<b>Constituent</b>	<b>Concentration (mg/L)</b>
H <sub>2</sub> SiO <sub>3</sub> *nH <sub>2</sub> O, silicic acid	15.3
KCl, potassium chloride	8.2
MgCO <sub>3</sub> , magnesium carbonate	13
NaCl, sodium chloride	15
CaSO <sub>4</sub> , calcium sulfate	67
CaCO <sub>3</sub> , calcium carbonate	150

Solutions for Iron Extractions

- Extract 1 reagent 1 M CaCl<sub>2</sub> in DIW
- Extract 2 reagent 0.5 M HCl: 12.9 mL concentrated HCl in 1.0 L DIW
- Extract 3 reagent 5.0 M HCl: 412 mL concentrated HCl in 1.0 L DIW
- Extract 4 reagent 0.25 M NH<sub>2</sub>OH·HCl: 1.74 g in 0.100 L DIW
- Extract 5 reagent dithionite-citrate-bicarbonate: 0.30 M NaC<sub>6</sub>H<sub>8</sub>O<sub>7</sub>, 1.0 M NaHCO<sub>3</sub>, and 0.06 M Na<sub>2</sub>S<sub>2</sub>O<sub>4</sub>

Solutions for Ferrozine Analysis Following Iron Extractions

- Ferrozine solution: 1.0 g ferrozine (CAS 69898, 3-(2- pyridyl)-5,6-bis(4-phenylsulfonic acid)-1,2,4-triazine, 494.37 g/mol) + 13 g HEPES, free acid pH buffer, in 1.0 L DIW for a final concentration of 0.002 M. Titration brought solution to pH = 7.
- Fe (II) standards: NIST traceable Fe(II) standard (1000 mg/L) used for typical standard curve of: 0.0, 0.10, 0.25, 0.50. 1.0, 2.0, 5.0, 10.0, 20.0, 30.0 mg/L in 0.15 M HCl.

*Batch Mineral Dissolution Experiments*

Twenty 120-mL anaerobic glass bottles labeled A-T were filled with ~2.0 g of sieved mineral. Then, ~60 mL of solution (either DIW or SGW depending on the sample) was added to the bottles and mixed at 120 rpm in a rotator (Cole-Palmer) for a solids concentration of ~33 g/L. Table 4 describes the conditions for each sample. Batch reactors were sampled at six different periods: 1 hour, 1 day, 3 days, 10 days, 30 days, and ~ 60 days.

As a baseline, all seven minerals were exposed to 3.1 M NH<sub>4</sub>OH (5% NH<sub>3</sub>) in DIW under anaerobic conditions (92% N<sub>2</sub>/8% H<sub>2</sub>). Five minerals (muscovite, montmorillonite, illite, epidosite and microcline) were also exposed to 0.01 M NaOH in DIW under anaerobic conditions. Samples under anaerobic conditions were kept inside an anaerobic, flexible vinyl glove box (Coy Laboratory Products) which was checked for oxygen and hydrogen. Using palladium catalysts, oxygen was kept below detection limits for the meter (model 10) and hydrogen was kept to at least 8%. In the same manner, four minerals (muscovite, montmorillonite, illite and epidosite) were also investigated under anaerobic conditions in the presence of DIW. It is important to note that both minerals muscovite and montmorillonite underwent all five conditions as previous studies with

these phyllosilicates indicated significant mineral dissolution [2]. In addition, cations have a high tendency to sorb to these muscovite and montmorillonite's surfaces [2,5].

The sampling process consisted of removing two aliquots of 4 and 1 mL, for major cation and ferrozine colorimetric analysis, respectively. Bottles were first centrifuged for 10 minutes at 3000 rpm (Sorvall Dupont RC5C) to allow for separation of the aqueous phase from mineral solid. Then, aliquots were extracted using a 10-mL syringe filter needle (0.20  $\mu$ m nylon filter) through the septa. The pH was monitored using a hand-held pH meter (Orion pH10series). A three-point calibration was completed prior to each use of the meter. Finally, samples were acidified to a concentration of 2%  $\text{HNO}_3$  for inductively couple plasma optical emission spectrometer (ICP-OES, Perkin Elmer 7300DV) analysis and 2%  $\text{HCl}$  for ferrozine analysis. All samples for ICP-OES analysis were sent to FIU-ARC for analysis for Si, Al, Fe, Na, K, Ca, and Mg with the help of Dr. Hilary Emerson. All samples containing U(VI) were sent to PNNL's building 331/174, Dr. Nik Qafoku's lab, for ICP-MS analysis.

**Table 4. Conditions and Sampling Events for Seven Hanford Site Minerals for Kinetic Dissolution Experiments (Note: letters represent the labels used for sample bottles)**

Mineral	Anaerobic DIW + 5% $\text{NH}_3$	Aerobic DIW + 5% $\text{NH}_3$	Anaerobic SGW + U + 5% $\text{NH}_3$	Anaerobic SGW + U + 5% $\text{NH}_3$ – 4 wk age then air strip to pH 8	Anaerobic DIW + 0.01 M NaOH
Muscovite	A	H	L	N	P
Montmorillonite	B	I	M	O	Q
Quartz	C				
Illite	D	J			R
Calcite	E				
Epidosite	F	K			S
Microcline	G				T

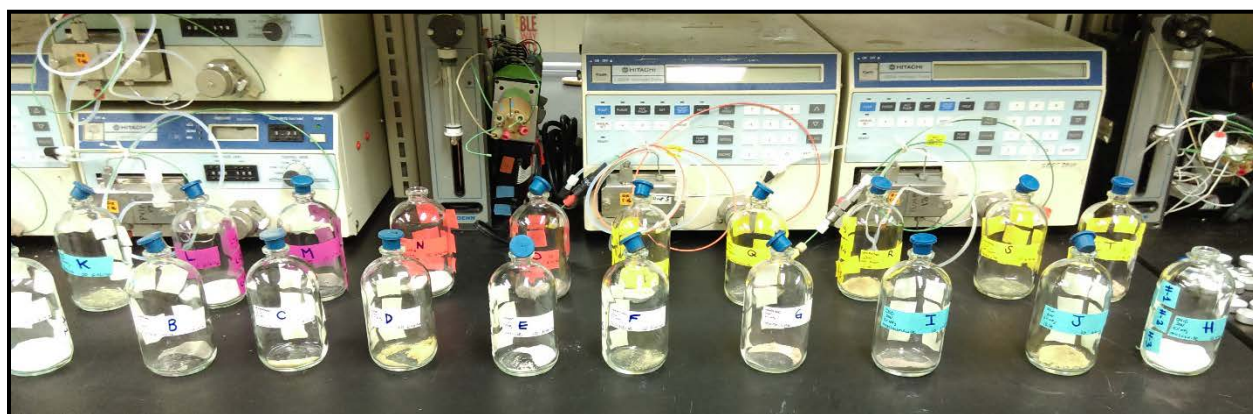


**Figure 4. Twenty glass bottles containing different Hanford minerals about to be capped with aluminum and septa for mineral dissolution experiment.**

### *Iron phase extractions*

Iron phase extractions were performed to quantify changes in available Fe(II) and total Fe mineral in six pure minerals (biotite, illite, epidosite, magnetite, muscovite, and montmorillonite). Table 5 depicts the reagents and time period for each iron phase extraction. For each of these extractions, ~2.0 g of mineral was mixed with 10 mL of reagent solution, mixed for the allotted time, centrifuged for 10 min. at 3000 rpm, and liquid filtered with a 0.45  $\mu\text{m}$  nylon syringe filter [10,11].

Analysis of total Fe and  $\text{Fe}^{2+}$  was performed by the ferrozine colorimetric method using a DR/4000 U Spectrophotometer (Figure 5) using Hach code 2175 [9]. Ferrozine [3-(2-pyridyl)-5,6-bis(4-phenylsulfonic acid)-1,2,4-triazine], shown in Figure 6, is a compound that reacts with divalent iron to form a stable magenta complex species. The species' high solubility allows for direct determination of iron in water via absorption in the visible range as a single, sharp peak at 562 nm [5,8]. The method detection limit was ~0.016 mg/L based on an average of each calibration curve as a new calibration curve was collected each time samples were analyzed (Figure 7, Appendix B).

Iron assay steps included pipetting 1.5 mL Ferrozine solution, 300  $\mu\text{L}$  of 0.15 M HCl, and 200  $\mu\text{L}$  of sample or standard into a 4.5-mL polystyrene cuvette. A period of 10 minutes was allowed for the ferrozine to complex with the Fe in the sample or standard. For total iron analysis, 0.5 mL of 0.25 M  $\text{NH}_2\text{OH}\cdot\text{HCl}$  was added to the aforementioned solution. Fe(III), if present, must be reduced to Fe(II) to produce the colored species (Eq. 1) [11]. The reagent used for this purpose is hydroxylamine hydrochloride,  $\text{NH}_2\text{OH}\cdot\text{HCl}$ .

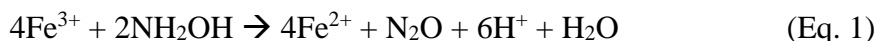


**Figure 5. Hach DR/4000 U spectrophotometer.**



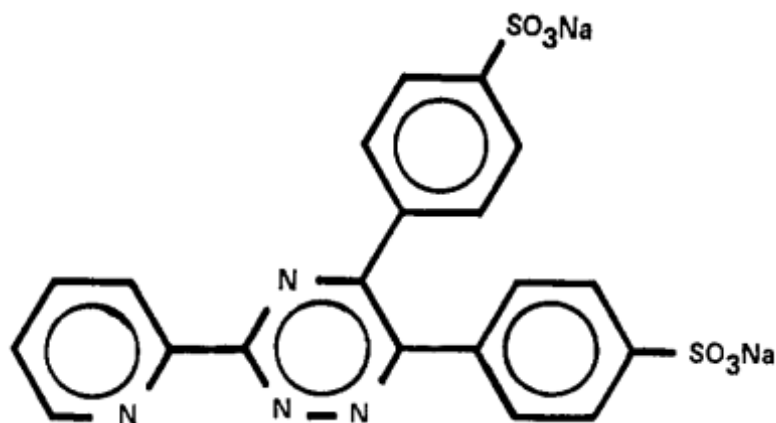


Figure 6. Structure of ferrozine.

Table 5. Reagent, Mixing Times and Target Phase for Iron Phase Extractions Extract 1-5 of Six Pure Minerals for Analyzed Species [11]

Extract	Reagent	Mixing Conditions	Target Phase	Analyzed Species
1	1.0 M CaCl <sub>2</sub>	50 min. (anaerobic)	Ion Exchangeable Fe(II)	Fe(II)
2	0.5 M HCl	24 hours	FeS, FeCO <sub>3</sub>	Fe(II)
3	5 M HCl	21 days	Fe(OH) <sub>3</sub> , FeOOH, Fe <sub>2</sub> O <sub>3</sub>	Fe(II), Fe(III), Total Fe
4	0.25 M NH <sub>2</sub> OH·HCl	30 min. at 50 °C	Amorphous and poorly crystalline Fe(III)	Total Fe
5	dithionite-citrate-bicarbonate	30 min. at 80 °C	Crystalline Fe(III)	Fe(II), Fe(III), Total Fe

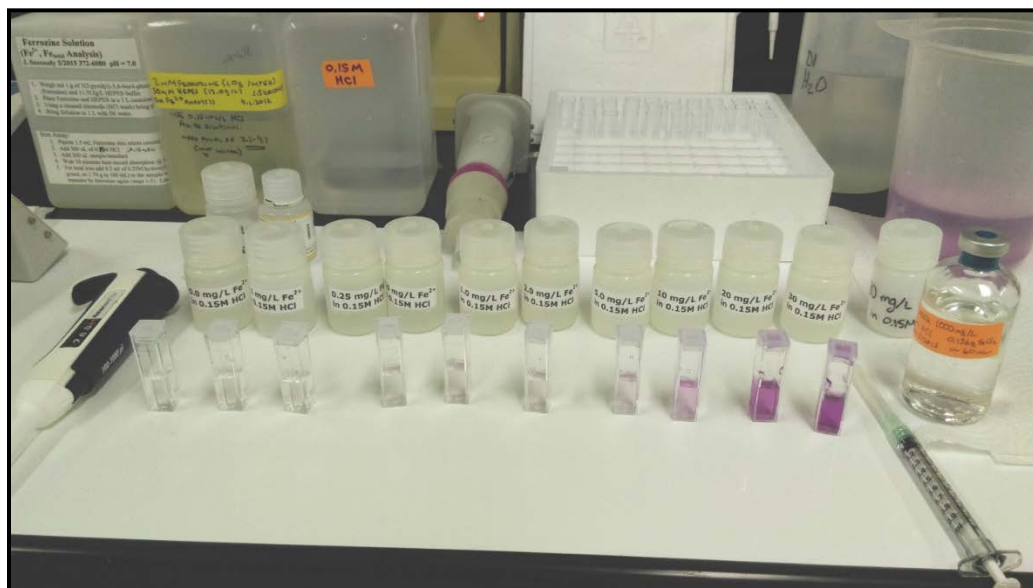
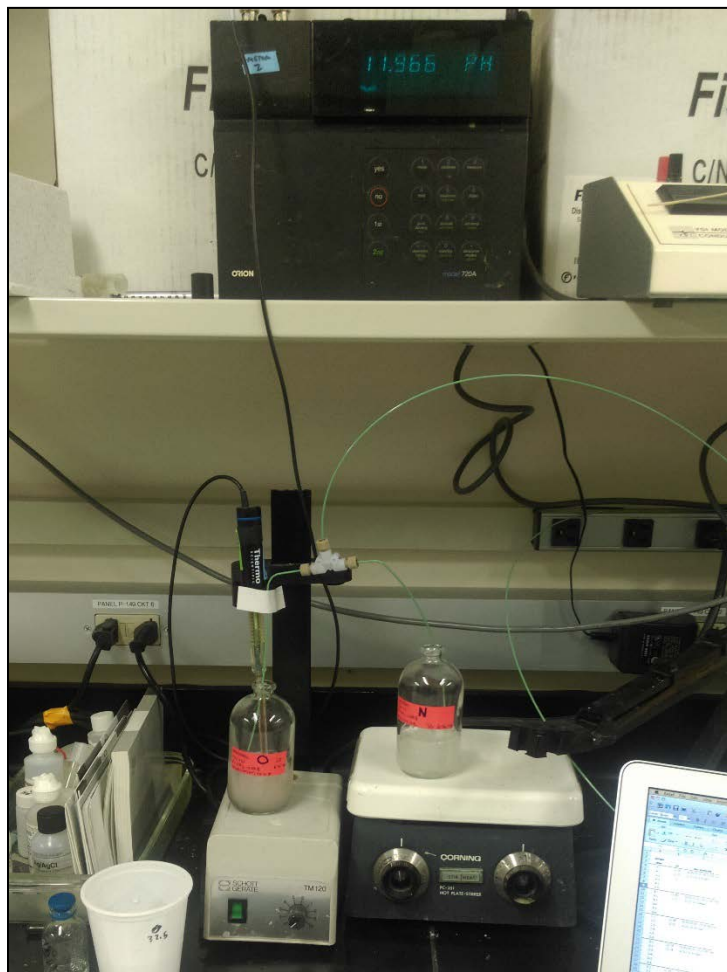


Figure 7. Ferrous ion standards used for ferrozine colorimetric analysis for iron phase extraction.



### *Air-stripping*

For uranium-spiked samples (N/O on Table 4), air-stripping was completed to determine the time until neutral pH was reached. This process allowed for aqueous  $\text{NH}_3$  to be removed from anaerobic batch reactors initially equilibrated with a 3.1 M  $\text{NH}_4\text{OH}$  SGW (synthetic groundwater) solution (Table 3). A small diameter plastic tube was inserted into the anaerobic bottle to inject compressed air (6.8 mL/sec). In addition, pH was continuously recorded during the air stripping process (ultra-semi micro Ross electrode, Thermo Scientific 8103BNUWP Orion 720A meter). Figure 8 represents the experimental setup for the air-stripping technique.



**Figure 8. Air-stripping technique for uranium-containing bottles N and O, with muscovite and montmorillonite respectively, with compressed air to reach neutral pH.**

## 4. RESULTS AND ANALYSIS

### *Mineral Dissolution*

Figures 9-12 represent results for aqueous Si in the presence of silica-containing minerals with respect to different conditions (Table 4). Figure 13 summarizes Si dissolved in units of  $\mu\text{molar}$  concentration per gram of all minerals analyzed when treatment condition anaerobic-DIW- $\text{NH}_4\text{OH}$  was applied.

### *Illite*

As Figure 9 shows, most dissolutions can be observed for the aerobic-ammonium hydroxide condition. For the first three sampling days ( $\sim 200$  hours or  $\log 0-2.4$ ), behavior is similar for all conditions with aerobic conditions showing the most dissolution while the control treatment  $0.01\text{ M NaOH}$  showed the least. However, after  $\sim 700$  hours ( $\log \sim 2.8$ ), the samples appear to have reached a plateau of  $\sim 18\text{ }\mu\text{M/g}$ . The exception is for the aerobic treatment where, at  $1000$  hours ( $\log 3.0$ ), aqueous Si concentration almost doubled ( $29\text{ }\mu\text{M/g}$ ).

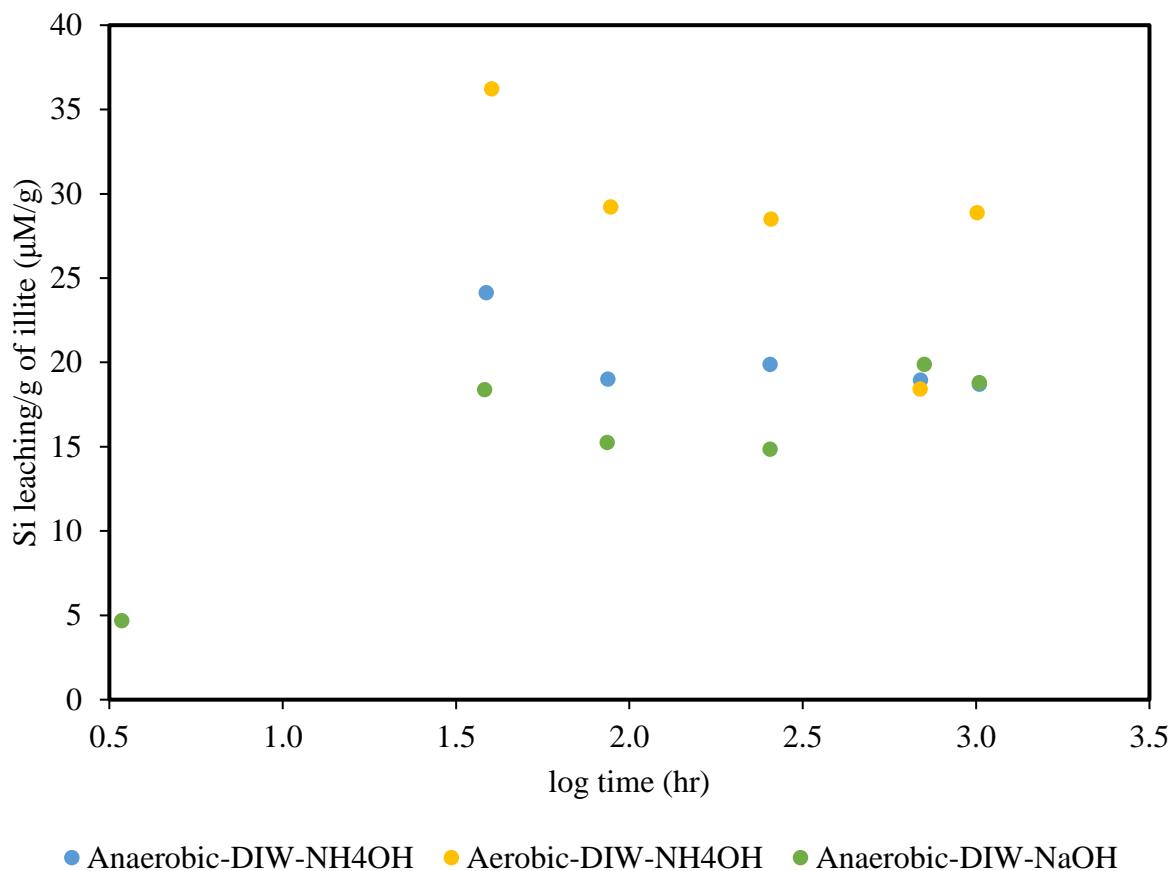


**Figure 9. Si leaching ( $\mu\text{M/g}$ ) versus time ( $\log \text{ hr}$ ) for illite.**

*Epidosite*

For the mineral epidosite, the dissolution behavior is similar to illite (Figure 9). Sampling days 1-3 (0-300 hours or log 1.6-2.4) show the same trend, with the aerobic-treatment condition showing the most dissolution. After sampling day 4 (700 hours or log ~2.8) of mineral-solution-contact time, dissolution is similar with the exception of anaerobic treatment showing the most dissolution at 56  $\mu\text{M/g}$ .

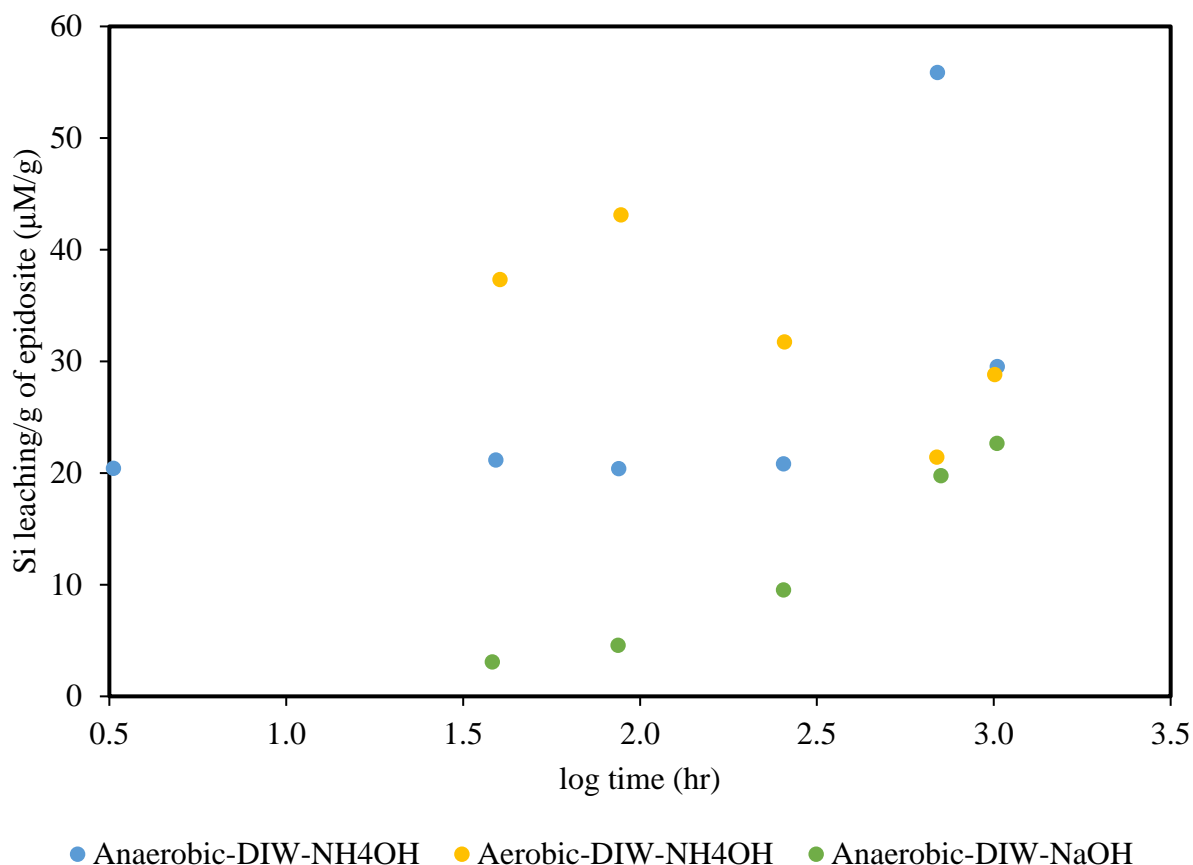


**Figure 10. Si leaching ( $\mu\text{M/g}$ ) versus time (log hr) for epidosite.**

*Muscovite*

Muscovite dissolution follows a similar trend as illite and epidosite, especially for the anaerobic-DIW-NaOH condition. Figure 11 shows the least Si leaching, or lowest dissolution, when muscovite minerals were in contact with a control solution of 0.01 NaOH. However, Si dissolved nearly less than half compared to illite and epidosite (the highest Si dissolution is seen at ~1000 hours or log 3.0).

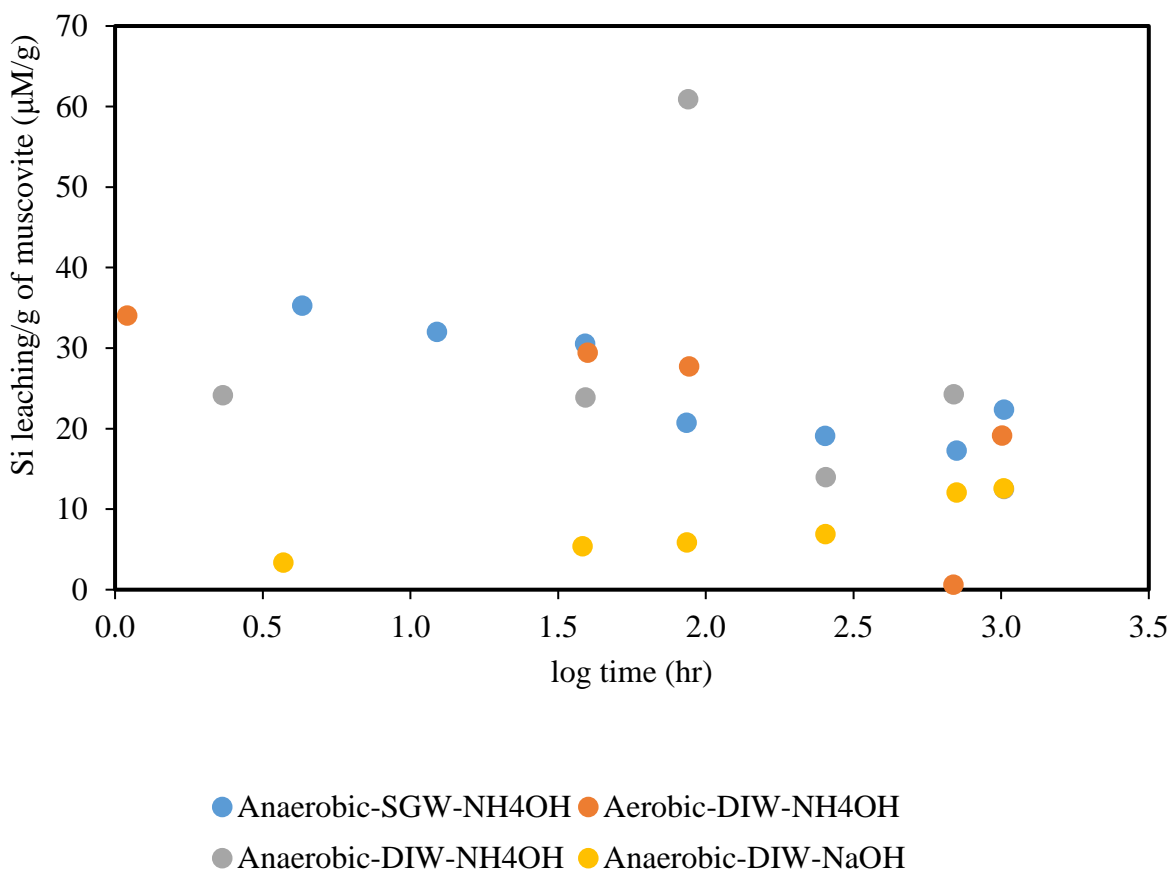


**Figure 11. Si leaching (μM/g) versus time (log hr) for muscovite.**

### *Montmorillonite*

Figure 12 shows montmorillonite mineral dissolution of Si undergoing four conditions as seen in Table 4. Unlike Figures 9-11, the treatment condition of ammonia gas, both anaerobic in SGW and DIW, show the lowest dissolution. It is particularly interesting that under anaerobic-SGW-NH<sub>4</sub>OH conditions, no dissolution was seen. Thus, further ICP-OES analysis will be performed. However, post-experiment BET analysis in Table 6 shows that montmorillonite's surface area almost doubled, from an initial surface of 9.82 m<sup>2</sup>/g to 16.8 m<sup>2</sup>/g. Contrary to muscovite's surface area, the post base treatment surface area increased only 20%. This could be due to montmorillonite's different ion exchange capacities or the chemical-structural arrangement of this expandable phyllosilicate.

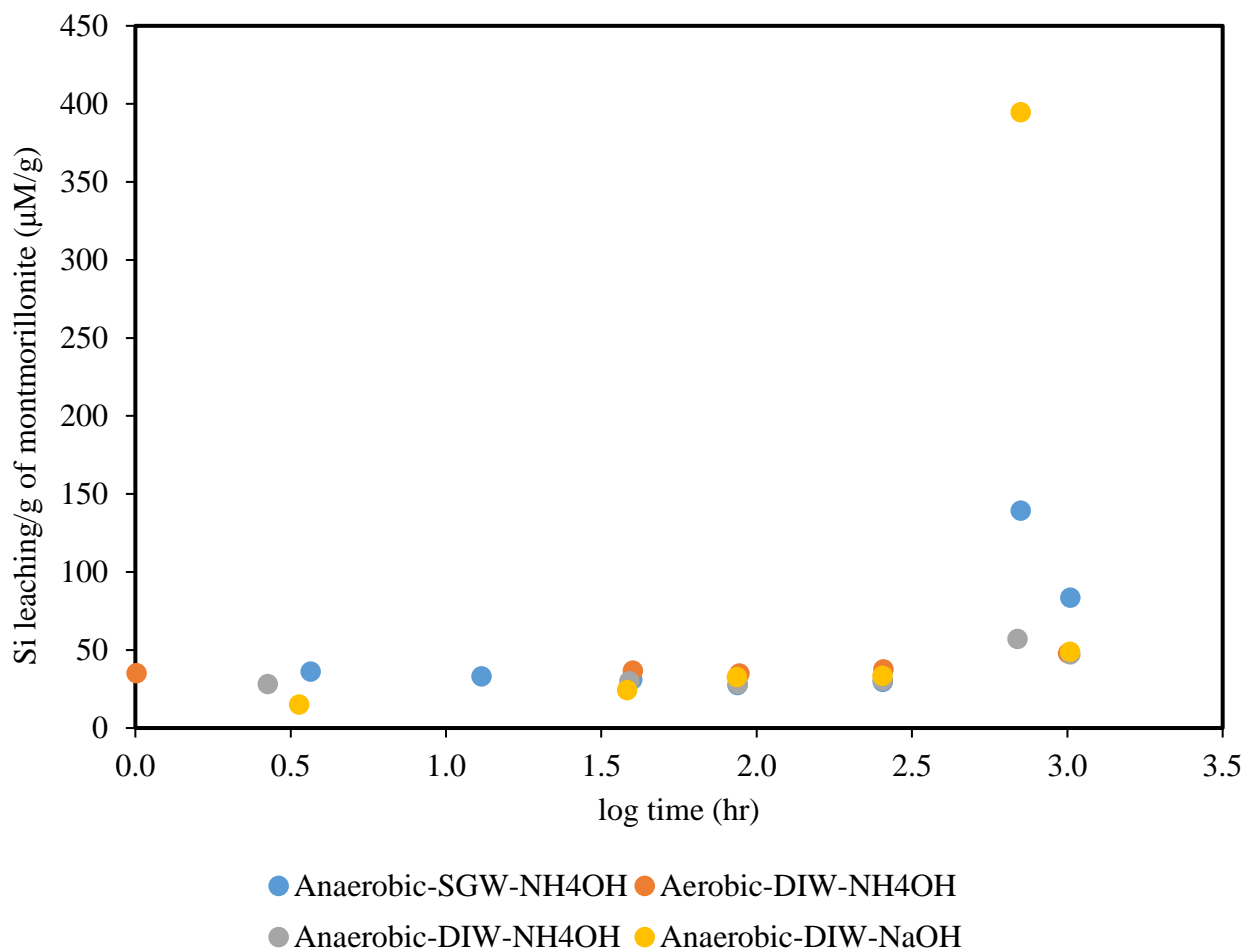


**Figure 12. Si leaching ( $\mu\text{M/g}$ ) versus time (log hr) for montmorillonite.**

Figure 13 summarizes six out of seven minerals (with the exception of calcite where no Si analysis was performed) that underwent the anaerobic-DIW-NH<sub>4</sub>OH condition. Although it is rather difficult to show any remarkable concluding statements, it can be noted that all minerals show a higher concentration of Si dissolution as a function of time. Exceptions are microcline and epidosite where these minerals show a high peak in dissolution after 80 hours (log 1.9) and 700 hours (log 2.85) of reaction-time, respectively, and then there is a decrease. Further analysis is needed to continue the investigation. However, one general conclusion that can be noted is that the longer the contact time, the different the dissolution capabilities depending on the mineral being analyzed. For example, for sampling day 1 (log 0.5), all minerals are clustered at a dissolution of  $\sim 20\text{--}30\ \mu\text{M/g}$ . As time progressed, mineral dissolution varied more widely, ranging from  $13\ \mu\text{M/g}$  in microcline to as much as  $47\ \mu\text{M/g}$  for montmorillonite.

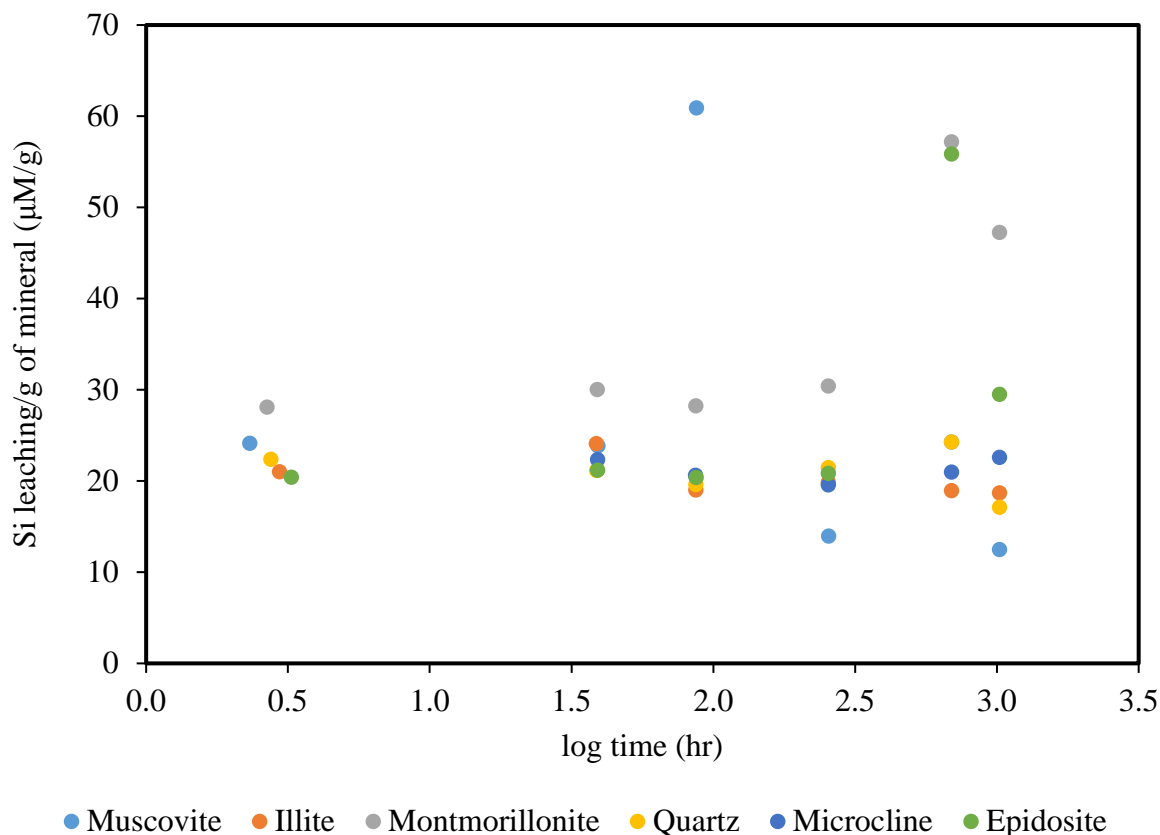


Figure 13. Mineral comparison of Si in anaerobic-DIW-NH<sub>4</sub>OH treatment condition as respect with time (log scale).

Table 6. Post Experiments BET Analysis

Mineral	Conditions	Average BET surface area, m <sup>2</sup> /g	Pore size, Å
Montmorillonite	Anaer/NH <sub>4</sub> OH	16.8	89.1
	Aer/NH <sub>4</sub> OH	17.0	90.9
	Anaer/NaOH	19.3	90.1
	Initial	9.82	104
Muscovite	Anaer/NH <sub>4</sub> OH	0.571	196
	Aer/NH <sub>4</sub> OH	0.797	196
	Anaer/NaOH	1.26	140
	Initial	0.67	211

#### Comparison of minerals

For U-spiked bottles L and M, the highest U concentration appears to be 18 ppm for muscovite (Figure 14) and 20 ppm for montmorillonite (Figure 15). Although peak concentration is similar for both, the time is not. For muscovite, U peak desorption was seen at sampling day 4 (86 hours),

while for montmorillonite, it was seen at sampling day 3 (40 hours) and then there is a significant plateau.

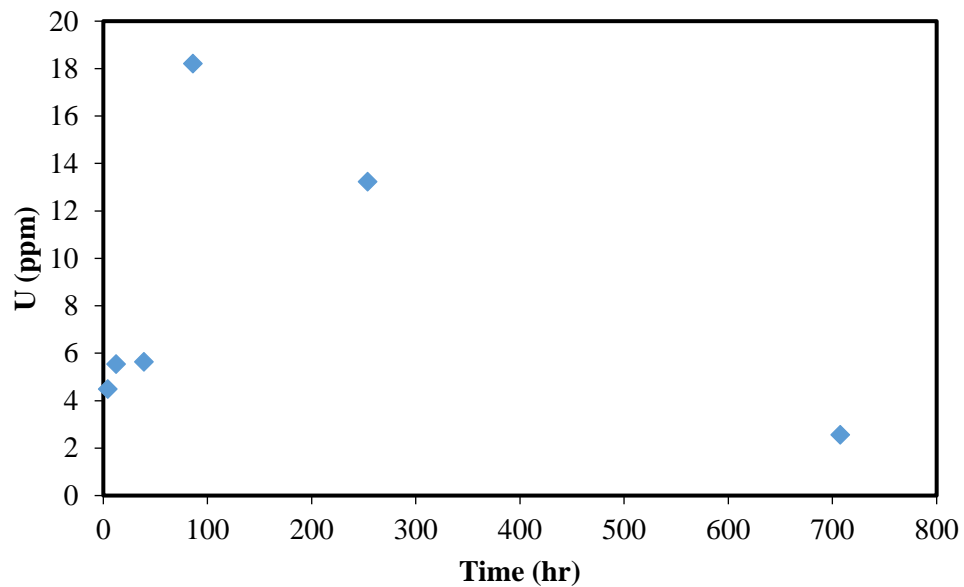


**Figure 14. Anaerobic SGW + 1ppm + bottle L in the presence of muscovite.**

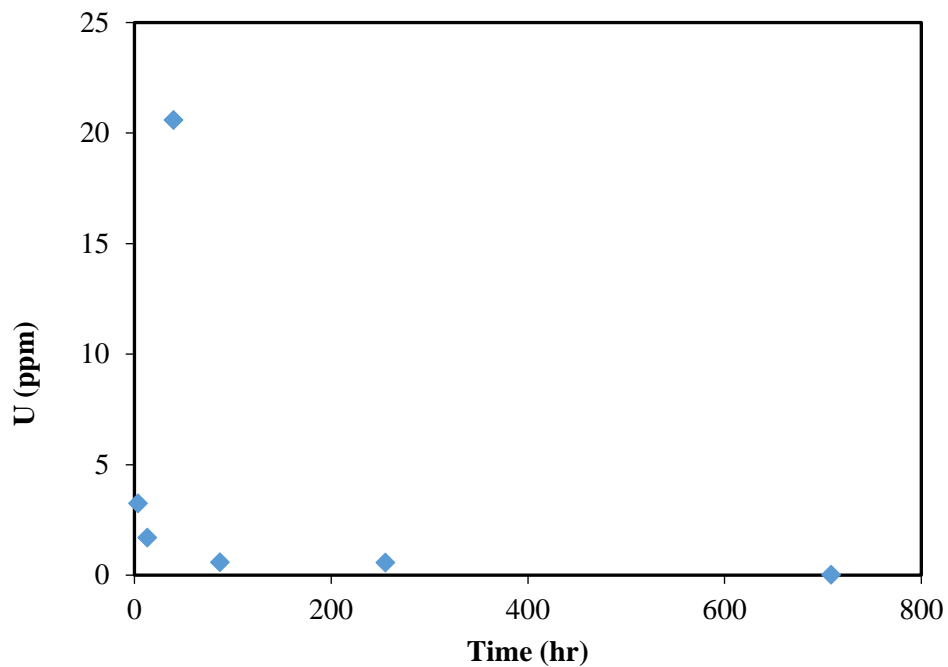


**Figure 15. Anaerobic SGW + 1ppm+ bottle M in the presence of montmorillonite.**

### Iron Phase Extractions

Figure 16 shows the ferrous/ferric ion ratio for all minerals analyzed in the iron phase extraction experiment. For extract 3 (5 M HCl, seen in blue), illite and montmorillonite show the lowest ratio, meaning that these minerals likely contain a high percentage of the Fe-(III)-oxidation state. On the other hand, biotite, showing the highest ratio, is likely to be readily found in the Fe-(II)-oxidation state. For extract 5 (0.25 M dithionite-citrate-bicarbonate), montmorillonite, epidosite and biotite show an equal amount of Fe (II) and Fe (III) oxidation states.

Figure 17 shows total Fe analysis for all six minerals. The highest total Fe concentration was seen for extract 3 – 5 M HCl. This is likely due to the higher contact time between the minerals and the reagent. As Table 5 indicates, the reaction time was 21 days. Furthermore, the high molarity of extract 3 may lead to more dissolution, which could be  $\text{Fe}(\text{OH})_3$ ,  $\text{FeOOH}$  and/or  $\text{Fe}_2\text{O}_3$  complexes.

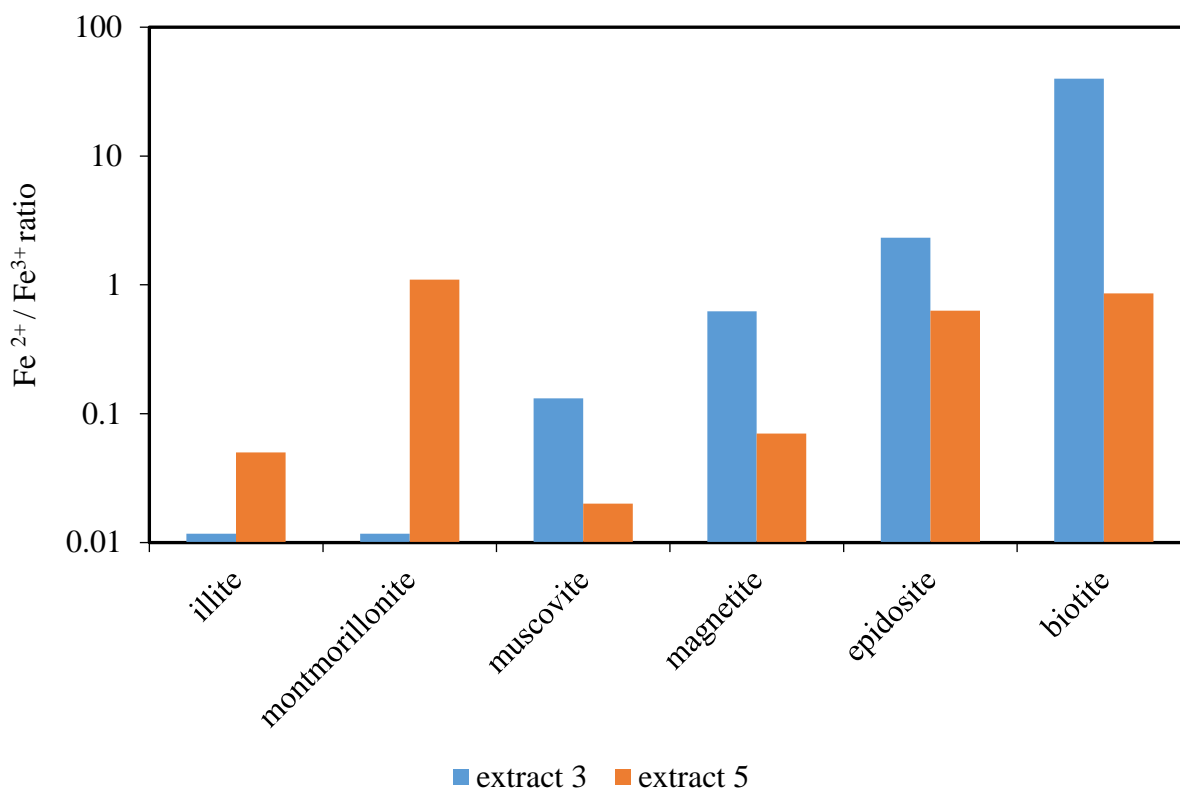


**Figure 16.** Ferrous ion / ferric ion ratio for extract 3 (5 M HCl) and extract 5 (0.25 M dithionite-citrate-bicarbonate).



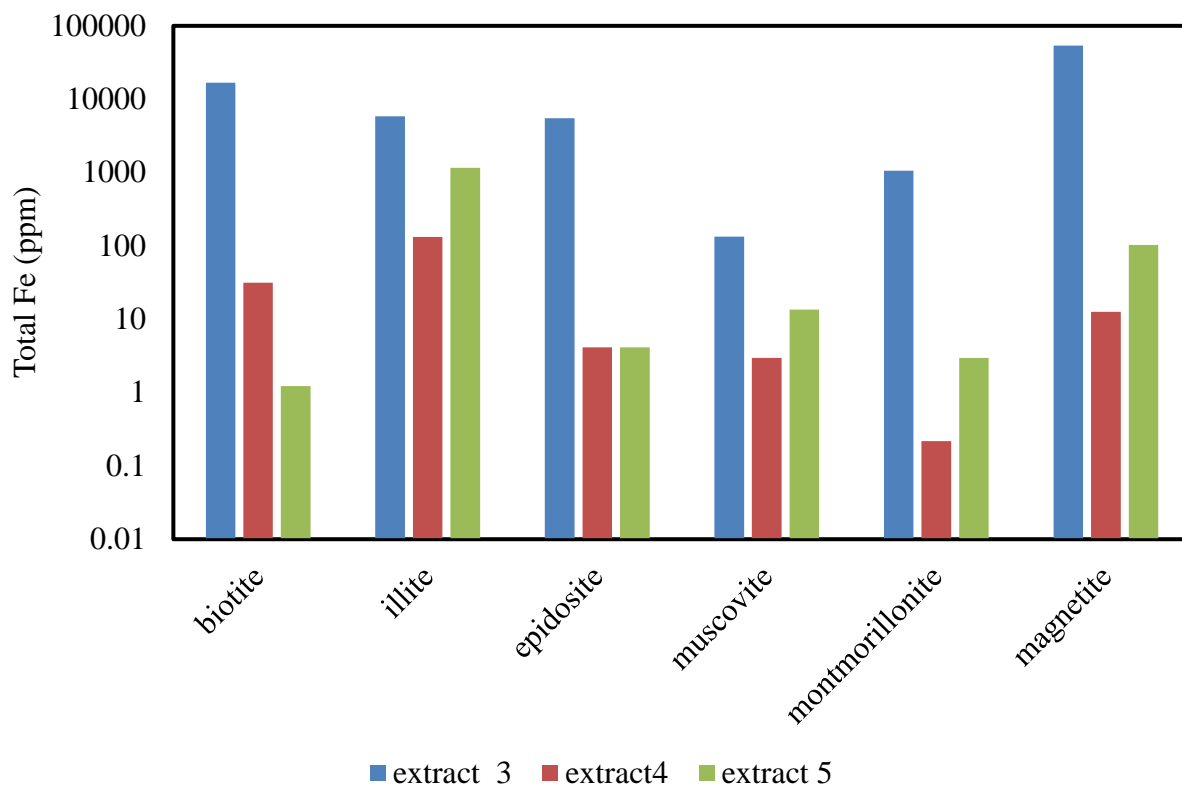


Figure 17. Total Iron for extract 3 (5 M HCl) and extract 5 (0.25 M dithionite-citrate-bicarbonate).

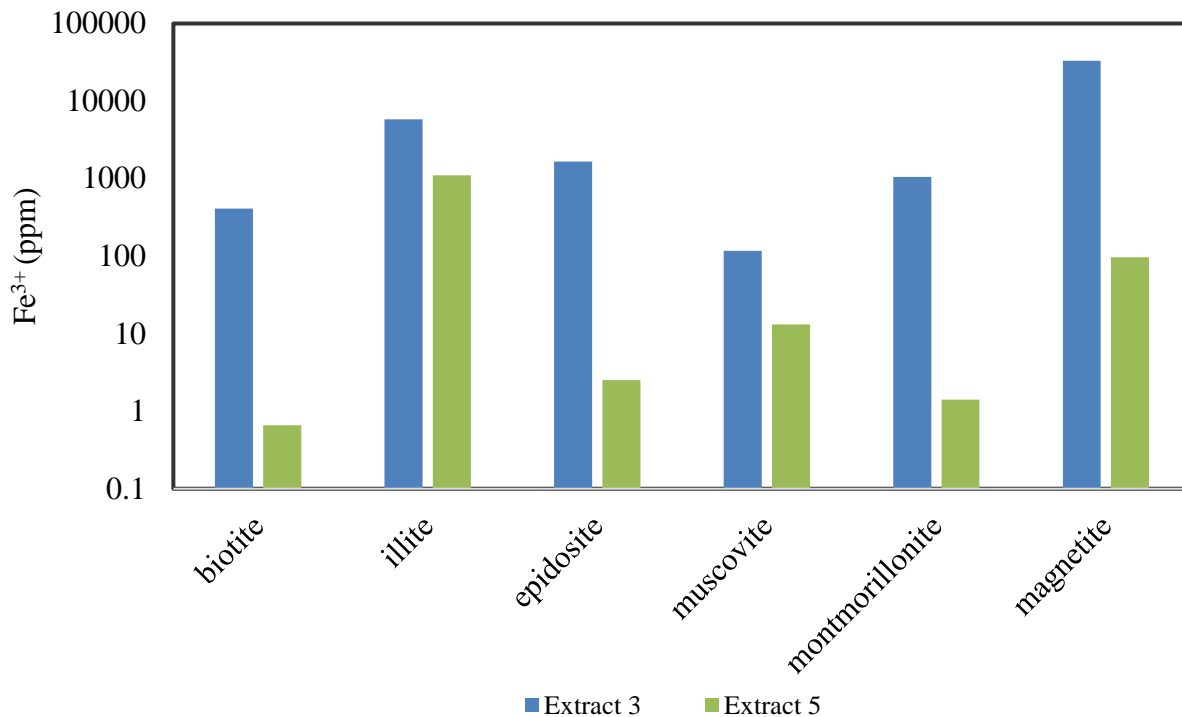
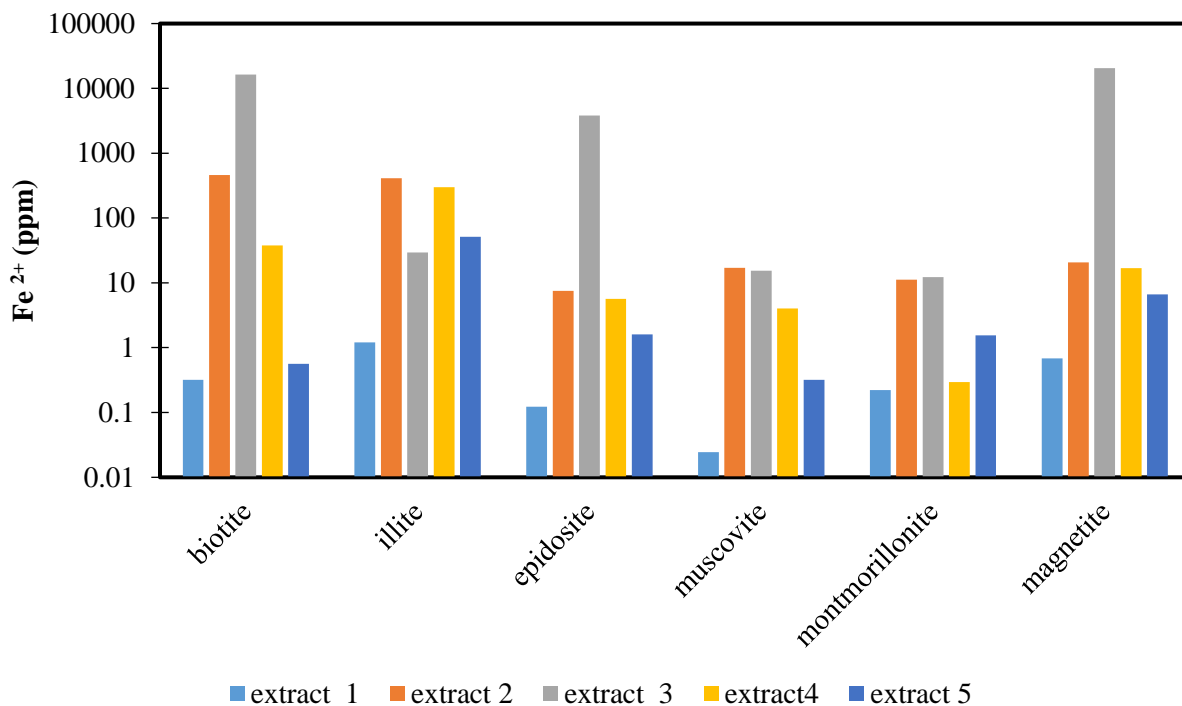


Figure 18. Ferric Iron - extract 3 (5 M HCl) and extract 5 (0.25 M dithionite-citrate-bicarbonate).



**Figure 19. Ferrous Iron (ppm) for all minerals analyzed in extract 1-5.**

### *Air-stripping*

Figure 20 shows the air-stripping technique being applied to U-containing bottles N and O, muscovite and montmorillonite, respectively. The technique, as seen in Figure 8, was applied during a period of 11,040 minutes, or approximately 7 and half days. During this period, muscovite reached a pH level of 8.13 and montmorillonite a pH of 8.69. Initial pH conditions were 12.1 and 12.4 for muscovite and montmorillonite, respectively.

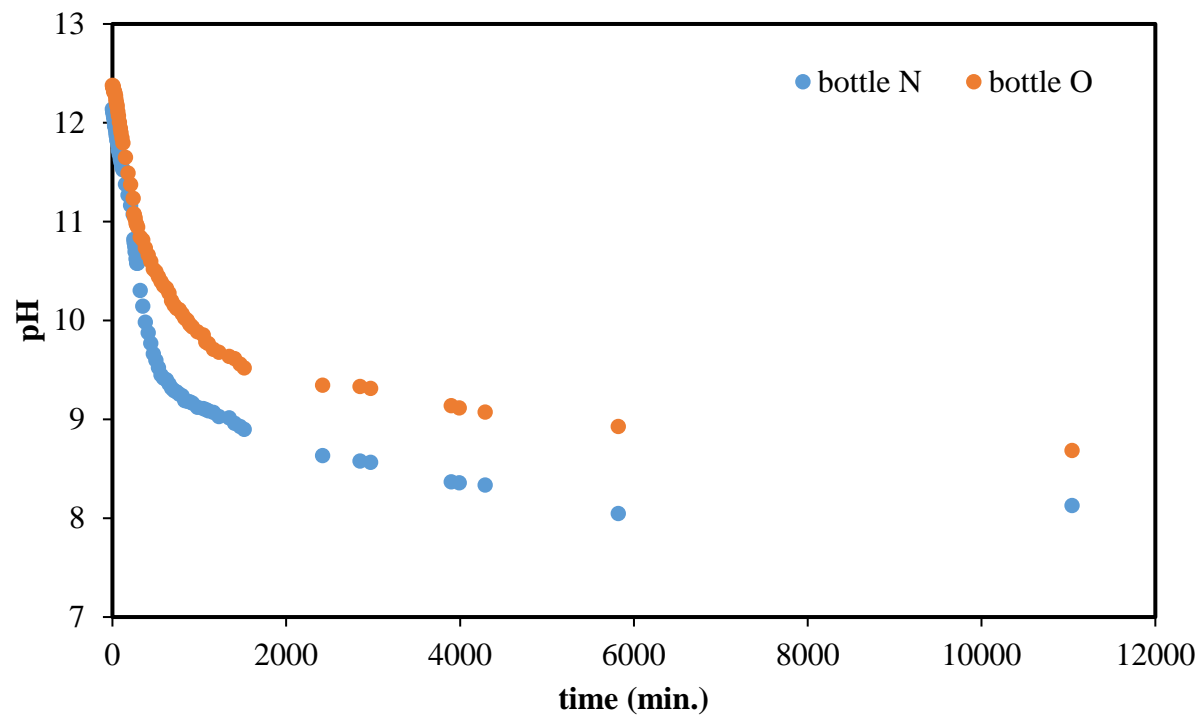


**Figure 20. Bottles N (blue) and O (orange) containing 3.1 M  $\text{NH}_4\text{OH}$  (5%  $\text{NH}_3$ ) solution air-stripped with compressed air to reach neutral pH as a function of time.**

## 5. CONCLUSIONS

---

Batch dissolution experiments were conducted using seven pure minerals. These were expected to dissolve under alkaline pH conditions. Table 4 summarizes the conditions that each mineral encountered. For epidosite, illite and muscovite, Si dissolution for three conditions is the same, where anaerobic-NaOH displays the lowest desorption and aerobic-NH<sub>4</sub>OH treatment the highest. Szecsody et al. found that ammonia gas injection is a potential technique that results in a large mineral-phase dissolution [13]. Therefore, the aerobic-NH<sub>4</sub>OH treatment results support the previous studies. For montmorillonite, however, the anaerobic-NH<sub>4</sub>OH in the SGW solution showed the lowest dissolution. Reasons for this could include montmorillonite's chemical properties, secondary phases coating the mineral's surface or faulty ICP-OES analysis.

However, the minerals epidosite, illite, muscovite and montmorillonite all show the highest dissolution for the aerobic-DIW-NH<sub>4</sub>OH condition. This result may lead to the conclusion that treatment exposed to atmospheric conditions is in fact a potential remediation technique that can be applied to the Hanford Site.

Further analysis is being conducted to determine the dissolution of other major cations for all seven minerals and to make comparisons among the treatments.

## 6. REFERENCES

---

1. Zachara, J. M., Brown, C., Christensen, J., Davis, J. A., Dresel, E., Liu, C., Um, W. (2007). A Site-Wide Perspective on Uranium Geochemistry at the Hanford Site.
2. Szecsody, J. E., Truex, M. J., Qafoku, N. P., Wellman, D. M., Resch, T., & Zhong, L. (2013). Influence of acidic and alkaline waste solution properties on uranium migration in subsurface sediments. *Journal of contaminant hydrology*, 151, 155-175.
3. Serne, J. (2012). Hanford Site Vadose Zone Sediment Mineralogy - Emphasis on Central Plateau. Richland, WA, Pacific Northwest National Laboratory.
4. Gee, G. W., Oostrom, M., Freshley, M. D., Rockhold, M. L., & Zachara, J. M. (2007). Hanford site vadose zone studies: An overview. *Vadose Zone Journal*, 6(4), 899-905.
5. McKinley, J. P., Zachara, J. M., Heald, S. M., Dohnalkova, A., Newville, M. G., & Sutton, S. R. (2004). Microscale distribution of cesium sorbed to biotite and muscovite. *Environmental science & technology*, 38(4), 1017-1023.
6. Xie, Y., Last, G. V., Murray, C. J., & Mackley, R. (2003). Mineralogical and bulk-rock geochemical signatures of Ringold and Hanford Formation sediments. *PNNL-14202. Prepared for the US Department of Energy*.
7. Serne, J. (2012). Hanford Site Vadose Zone Sediment Mineralogy - Emphasis on Central Plateau. Richland, WA, Pacific Northwest National Laboratory.
8. Serne, R. J., G. V. Last, G. W. Gee, H. T. Schaef, D. C. Lanigan, C. W. Lindenmeier, M. J. Lindberg, R. E. Clayton, V. L. Legore and R. D. Orr (2008). Characterization of vadose zone sediment: Borehole 299-E33-45 near BX-102 in the B-BX-BY waste management area, Pacific Northwest National Laboratory (PNNL), Richland, WA (US).
9. Stookey, L. L. (1970). Ferrozine---a new spectrophotometric reagent for iron. *Analytical chemistry*, 42(7), 779-781.
10. Chao, T. T., and Liyi Zhou. "Extraction Techniques for Selective Dissolution of Amorphous Iron Oxides from Soils and Sediments". *Soil Science Society of America Journal* 47.2 (1983): 225.
11. Heron, Gorm., Catherine. Crouzet, Alain C. M. Bourg, and Thomas H. Christensen. "Speciation of Fe(II) and Fe(III) in Contaminated Aquifer Sediments Using Chemical Extraction Techniques." *Environmental Science & Technology Environ. Sci. Technol.* 28.9 (1994): 1698-1705.
12. Sandell, E. B. (1945). Colorimetric Determination of Traces of Metals. *Soil Science*, 59(6), 481.
13. Szecsody, J. E., Truex, M. J., Zhong, L., Johnson, T. C., Qafoku, N. P., Williams, M. D., Faurie, D. K. (2012). Geochemical and geophysical changes during ammonia gas treatment of vadose zone sediments for uranium remediation. *Vadose Zone Journal*, 11(4), 0158, 13.

## APPENDIX A

---

**Table 7. Average pH for Mineral Dissolution Experiment Bottles A-T**

<b>Sample ID</b>	<b>Average</b>	<b>StDev</b>
A	12.20	0.02
B	12.45	0.05
C	12.31	0.08
D	12.18	0.05
E	12.20	0.05
F	12.23	0.09
G	12.17	0.04
H	12.39	0.10
I	12.66	0.09
J	12.37	0.10
K	12.43	0.08
L	12.27	0.06
M	12.49	0.12
N	12.22	-
O	12.34	-
P	12.48	0.15
Q	12.25	0.25
R	12.30	0.09
S	12.31	0.06
T	12.28	0.08
<b>Overall</b>	<b>12.33</b>	<b>0.16</b>

Note: bottles N and O underwent the air-tripping technique and were only sampled once.

## APPENDIX B

### *Limit of Detection – Mineral Dissolution*

To determine the limit of detection for elemental analysis in the mineral dissolution experiments, a calibration curve was developed based on the known concentration of the standards and the response (intensity) from the ICP-OES detector. Figure 21 shows an example for magnesium analysis with the average concentration on the y-axis and concentration in the x-axis as seen in Table 8. Once the values are plotted, an equation of the line in the form of  $y=mx+b$  is given. At the same time, Excel formula =STEYX is used to calculate the *standard error* of the detector response (Table 8). The value obtained is divided by  $m$ , or slope value, and thus the limit of detection (LOD) is obtained.

- Sample calculation:  $39451.8$  (standard error)  $\times 3.2 \div 1599.1$  (slope) =  $81.42$  (LOD).  
Because samples were diluted by a factor of 50, dilution corrected LOD becomes 4071.

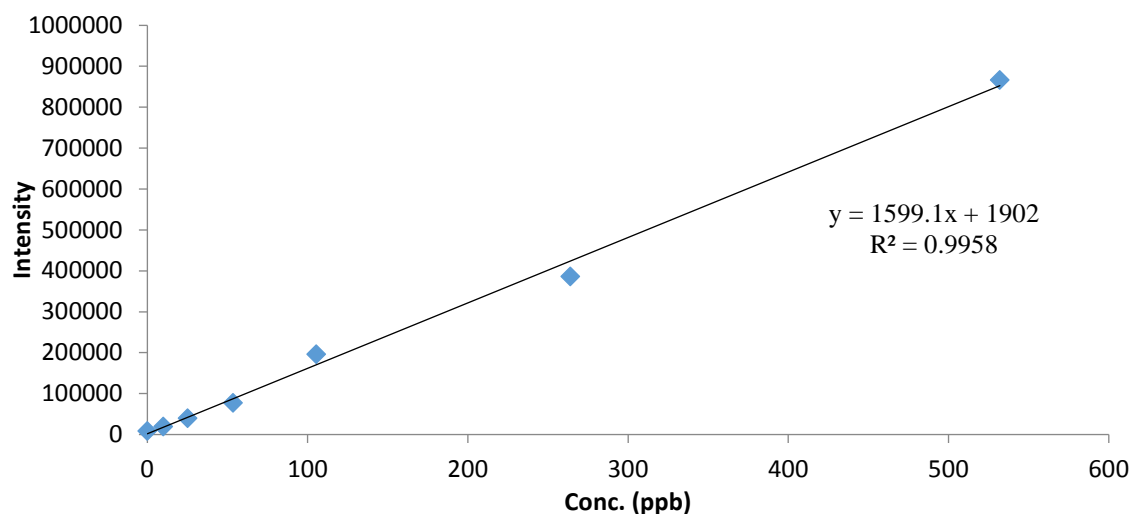


**Figure 21. Sample magnesium calibration curve for mineral dissolution run by ICP analysis.**

**Table 8. Standard Concentration and Average Intensity for Magnesium Calibration Curve**

<b>Std Conc. (ppb)</b>	<b>Average Intensity</b>
0	0
10	8672
25	19657
54	39992
105	77378
264	196487
532	386827
929	867002
<b>standard error</b>	39452
<b>slope</b>	1599
<b>LOD (ppb)</b>	81.42
<b>dilution corrected LOD(ppb)</b>	4071

*Limit of Detection – Iron Phase Extraction*

To determine the total iron and ferrous iron concentration, a standard calibration curve was performed before each analysis. Once detection was done using a Hach DR/4000 U spectrophotometer (Figure 5), the absorbance value was put into the equation of the line in the form of  $y=mx+b$  for a particular standard calibration curve (Figure 22).

- Sample calculation: if the value for absorbance was 0.031, plugging this into  $x$  using the equation from Figure 23, it would give a  $y$ -value of 0.693 mg/L  $\text{Fe}^{2+}$ . If this sample had been diluted, it was multiplied by the dilution factor. To determine the limit of detection for such samples, the  $x$ - and  $y$ -axis were inversed as seen in Figure 23. The  $b$  value obtained from the equation of the line in  $y=mx+b$  form, in this case 0.057 absorbance units, indicates the lowest detection, or absorbance reading, limit.



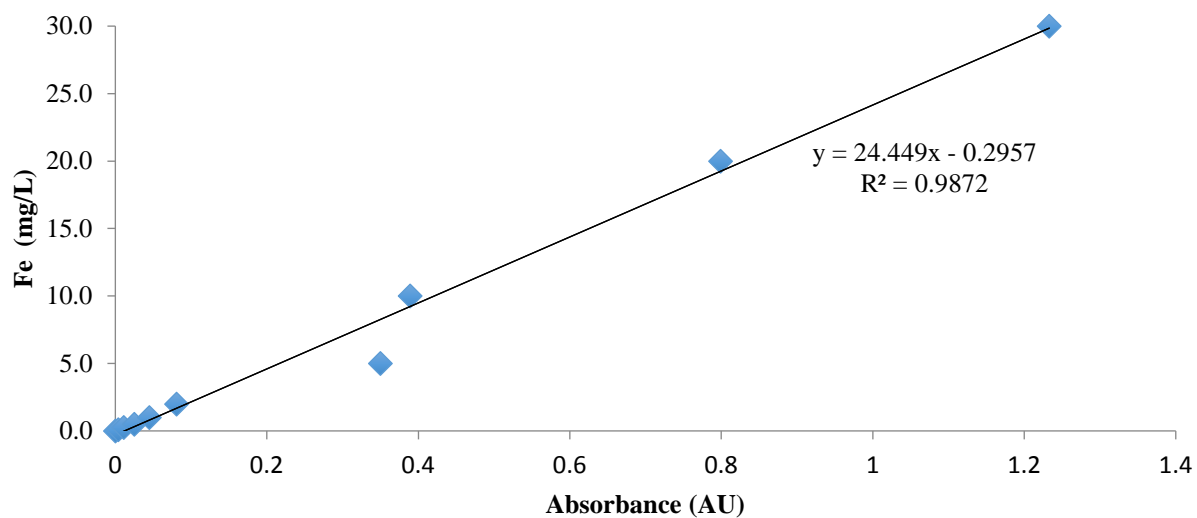


Figure 22. Sample of total iron calibration curve and its equation of the line for iron phase extraction analysis.

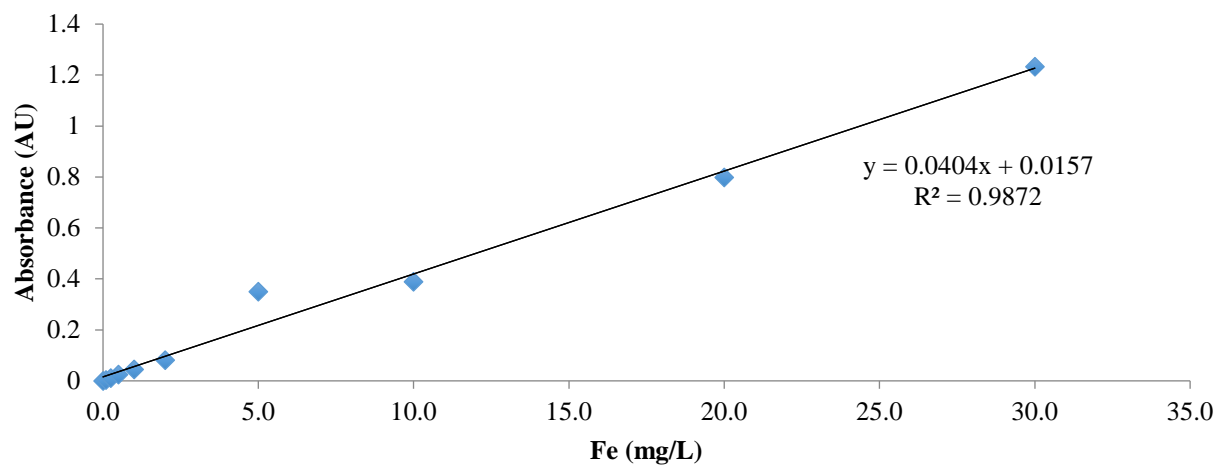
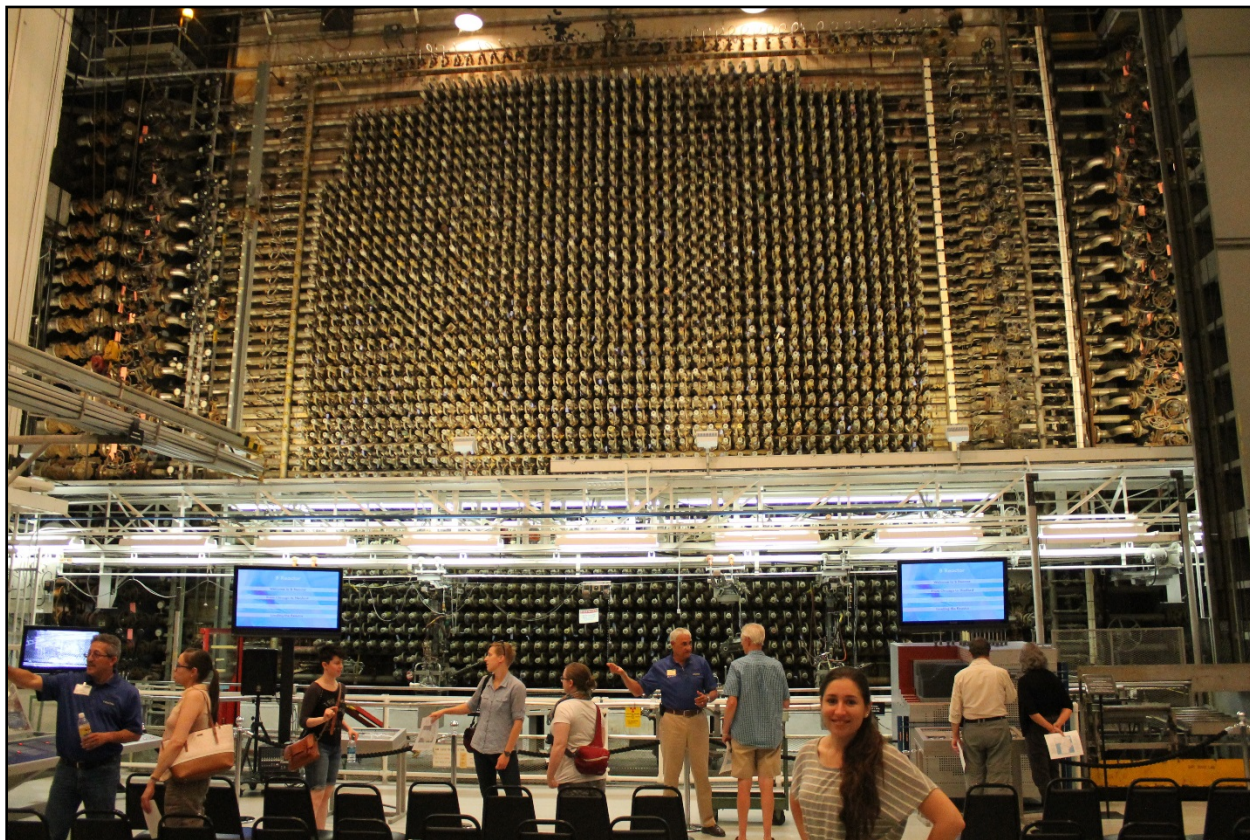


Figure 23. Sample of total iron calibration curve to determine limit of detection based on calibration curve from Figure 22.

## APPENDIX C

---

As part of the Alternative Sponsored Fellow internship program at PNNL, interns had the chance to tour the world's first nuclear production B-reactor "Manhattan Project" at Hanford's 200 Area. This was a wonderful opportunity not only to admire the magnitude of the reactor's engineering, but also to understand how and why this research is appropriate and useful to the Hanford Site.



**Figure 24. National Historic Landmark Nuclear Production Plant B-reactor constructed in 1943-1944.**

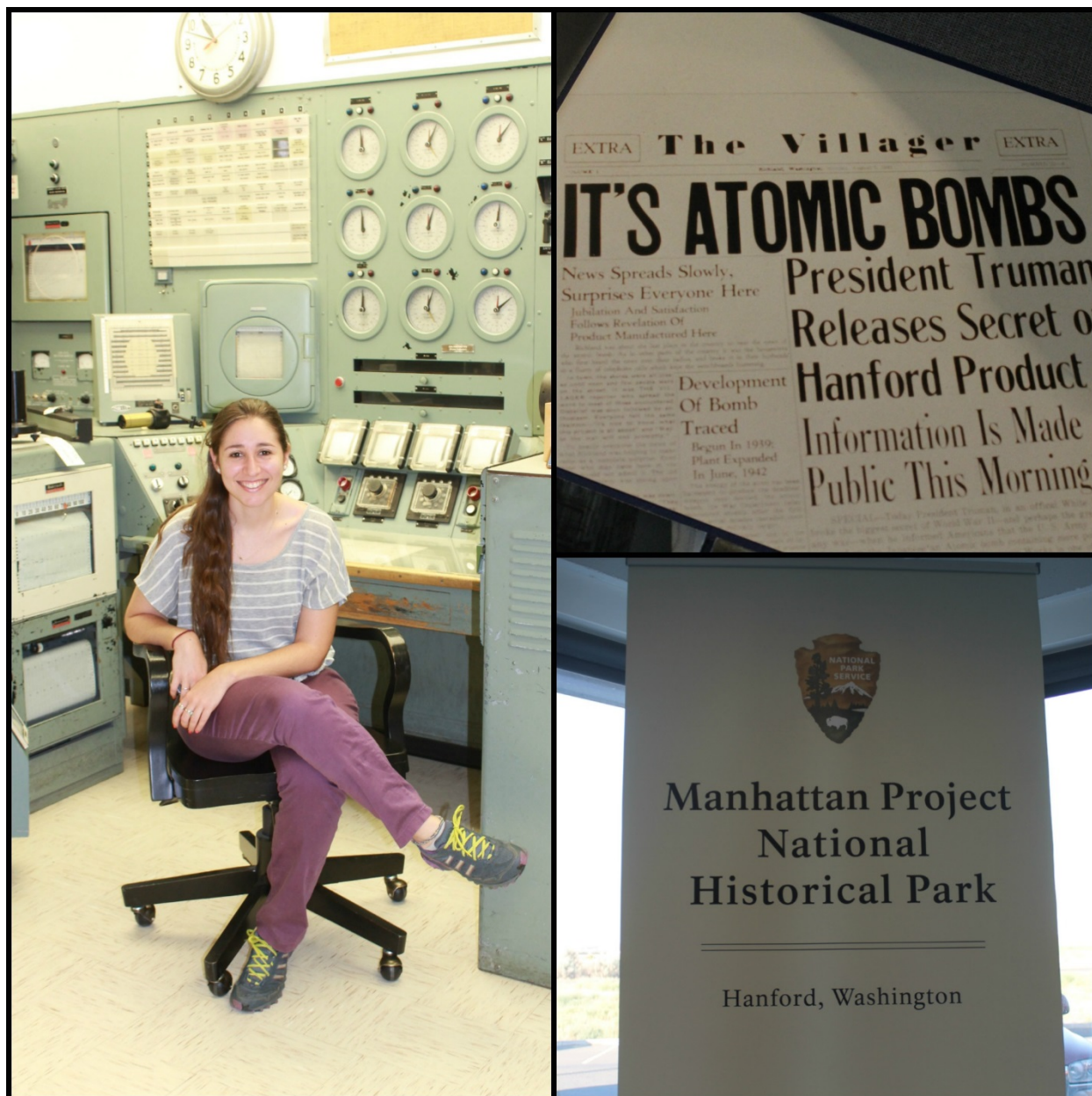
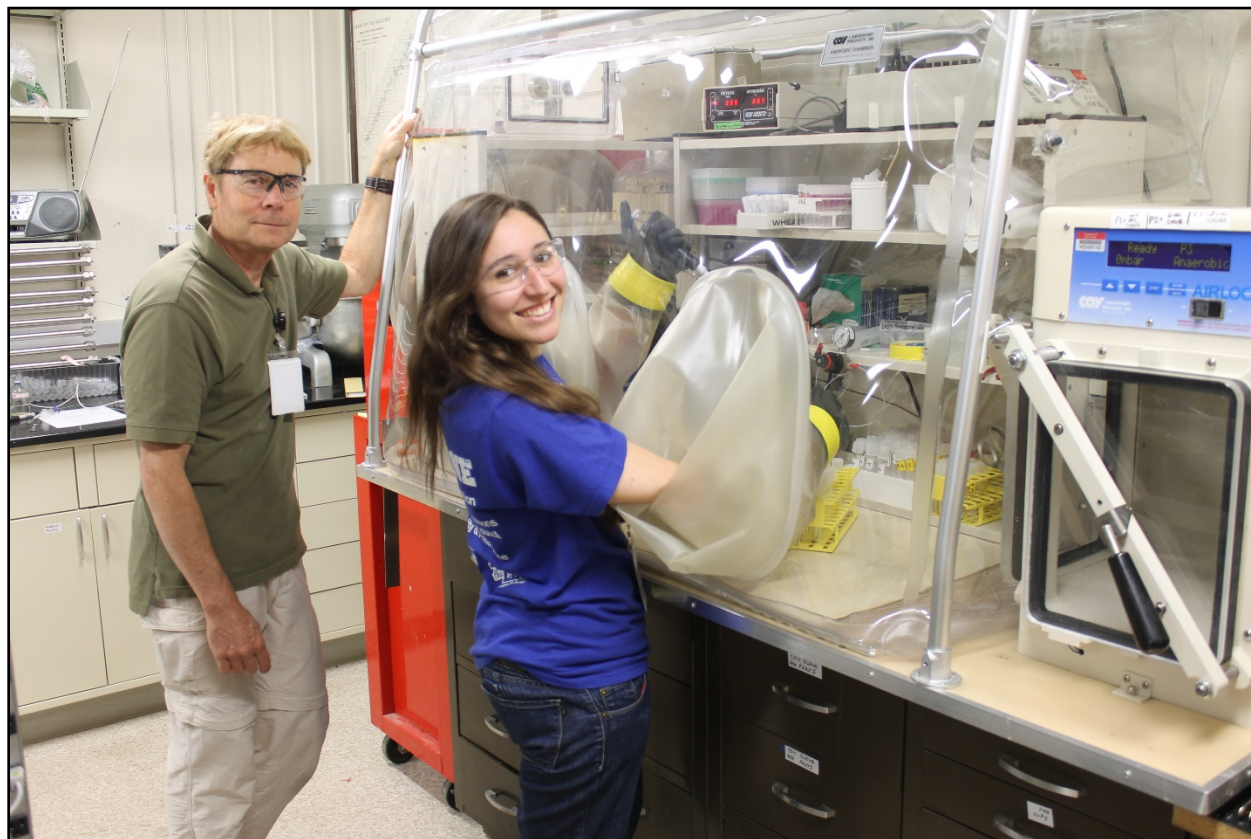


Figure 25. Silvina at B-reactor's control room and signs around the national landmark.



Silvina A. Di Pietro would like to thank Drs. Jim Szecsody and Nik Qafoku for their invaluable support and guidance throughout the duration of the internship at PNNL Building 331.



**Figure 26. With Dr. Jim Szecsody, lead scientist at the PNNL environmental system group, in his lab.**

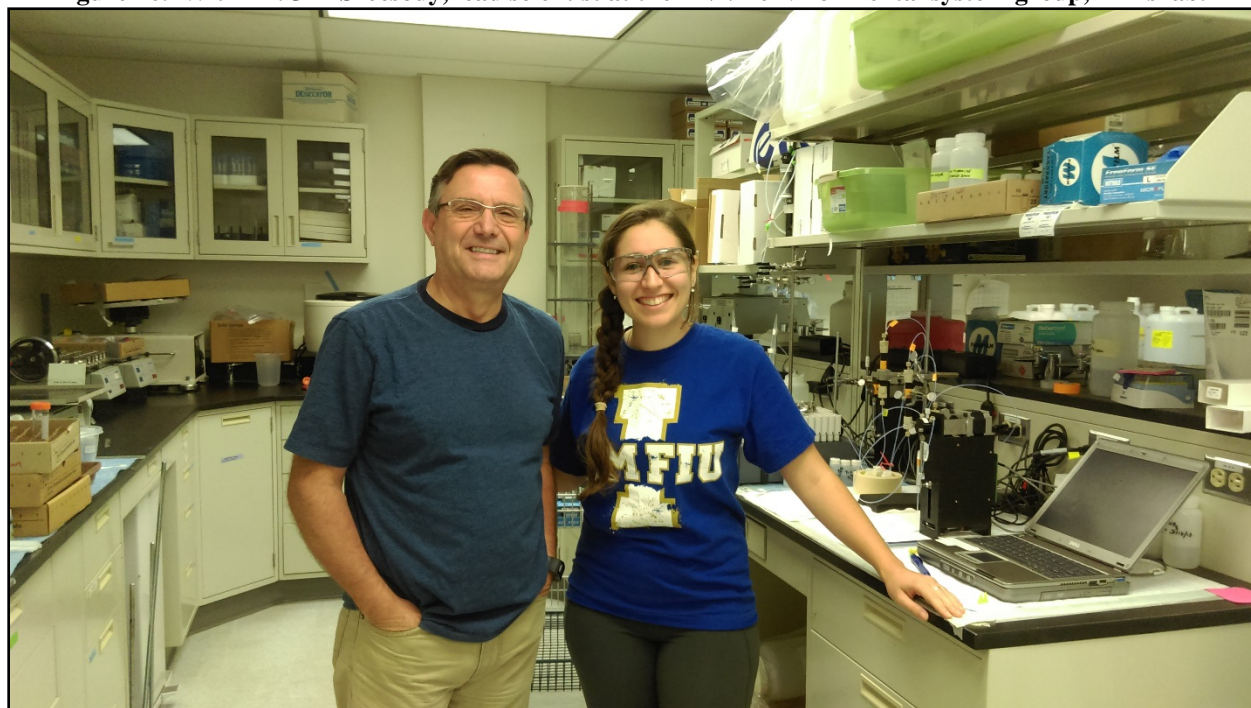


**Figure 27. With Dr. Nik Qafoku, chief senior scientist of PNNL's geosciences group, in his lab.**



**Figure 18. Silvina at PNNL's main entrance.**